# The Influence of Fluid Velocity on the Heat Transfer Coefficient of a Heat Collection System

**Lu Wei[1], Liang Lirui[1], Shi Dawei[2], Hou Yanhua[2], Zheng Yangxia[1], Jiang Chengyao[1], Li Mengyao[1], Yang Qichang[2], Tang Xiaopei[1,*]**

[1]College of Horticulture, Sichuan Agricultural University, Chengdu 611130, China
[2]Xinjiang Shengshi Huaqiang Agricultural Technology Co., Ltd, Hetian 848000, China

**Abstract:** In order to explore the influence of water velocity on the heat collection performance of the active heat storage and release system for solar greenhouses in Xinjiang province, six different flow rates were selected for treatment in this experiment. The comprehensive heat transfer coefficient of the active heat storage and release system at the heat collection stage was calculated by measuring the indoor solar radiation intensity, indoor air temperature and measured water tank temperature. The prediction model of water temperature in the heat collection stage was established, and the initial value of water temperature and the comprehensive heat transfer coefficient were input through MATLAB software. The simulated value of water temperature was compared with the measured value and the results showed that the best heat transfer effect could be achieved when the water flow speed was 1.0 $m^3 \cdot h^{-1}$. The average relative error between the simulated water tank temperature and the measured value is 2.70% ~ 6.91%. The results indicates that the model is established correctly, and the variation trend of water temperature can be predicted according to the model in the heat collection stage.

**Keywords:** Active Heat Storage and Release; Water Velocity; Heat Transfer Coefficient; Modeling; Solar Energy

**DOI:** 10.57237/j.jaf.2024.04.004

## 1 Introduction

Solar greenhouses are currently one of the most widely used horticultural facilities in China. With the advancement of modern agricultural technology, horticultural vegetable cultivation in solar greenhouses has developed, making a positive contribution to increasing farmers' incomes, promoting rural development, and enhancing agricultural efficiency in northern and high-altitude cold regions. [1, 2] It has become an essential component of modern agricultural production. [3] In recent years, the rapid development of modern agriculture in China has been moving towards trends of energy efficiency and high productivity. Although traditional heating methods in solar greenhouses (such as pipe heating, flue heating, and hot air heating) meet the heating needs during winter, they

Funding: Supported by the National Natural Science Foundation of Sichuan Province (2022NSFSC1645);
Key R&D Program Project of Xinjiang Province (2023B02020);
National agricultural science and technology innovation system Sichuan Characteristic Vegetable Innovation Team Project, the earmarked fund for Sichuan Innovation Team Program of CARS (SCCXTD-2024-22).

*Corresponding author: Tang Xiaopei, 18701068928@163.com

Received: 11 October 2024; Accepted: 8 November 2024; Published Online: 5 December 2024 http://www.agrforestry.com

are associated with high energy consumption, low heating efficiency, and environmental pollution. Due to the continuous depletion of fossil fuels and the emission of greenhouse gases such as carbon dioxide, the efficient utilization of clean energy and the reduction of energy consumption have become important areas of research in greenhouse development. As the number of greenhouses in the country continues to grow, the demand for heating in winter horticultural facilities is also increasing. [4] Maximizing the use of solar energy for photothermal conversion in solar greenhouse heating has been the focus of significant research. Scholars, both domestically and internationally, have conducted extensive studies on the selection, preparation, encapsulation of phase change materials, as well as their integration with greenhouse systems. [5] Therefore, it is important to explore low-carbon, efficient and energy-saving heating technologies for the healthy and sustainable development of facility horticulture.

Over the past decades, most of the domestic greenhouse wall research direction is focused on improving the structure of the wall itself, selecting more suitable materials, so that the greenhouse insulation and heat storage capacity is constantly improved. [6-9] Overall, most solar greenhouses in China still utilize passive heat storage methods for thermal insulation and retention. Due to harsh environmental conditions in winter, the temperature required for plant growth is significantly higher than the indoor temperature. To achieve better heat retention, some greenhouse owners have increased the thickness of the greenhouse walls. However, due to the inherent limitations of the wall materials, the heating effect is limited, leading to considerable resource waste. Due to the limited heat storage capacity of greenhouses, temperatures tend to be lower in the latter part of the night during extreme cold temperatures. To achieve optimal thermal insulation and heat retention performance, an ideal back wall should be composed of a heat-retaining layer and an insulating layer. [10, 11] However, such wall structures face challenges, including high construction costs and uncontrollable heat dissipation. In response to these challenges, it is imperative to develop and utilize alternative renewable energy sources to establish new winter heating methods for greenhouses. This approach will not only conserve energy and land resources but also alleviate the pressures associated with energy scarcity.

To enhance the utilization of solar clean energy, Yang Qichang et al. [12-14] proposed the concept of an active heat storage and release system. This approach involves utilizing the greenhouse's own structure or properties to absorb and store solar radiation during the day, and subsequently releasing the stored heat during the night or winter when needed. This method improves the efficiency of solar energy utilization and facilitates the transfer of heat in both spatial and temporal dimensions, thereby transforming the passive thermal storage and release of greenhouses into an active system. Fang Hui [13] et al. utilized heat exchange pipes to collect solar energy, storing the heat in shallow soil. At night, the stored heat is naturally released from the shallow soil to warm the greenhouse. Zhang Yi [14] et al. and Liang Hao [15] et al. employed fluid mediums to achieve active thermal energy storage and release. Sun Weituo [16] et al. and Zhou Sheng [17] et al. integrated the Active Heat Storage and Release System (AHS) with heat pumps for application in greenhouses. Other studies include the evaluation of energy-saving thermal insulation performance based on the active heat storage and release system, investigations into the environmental factors affecting the system's heat collection and release [18], and modeling and analysis of the greenhouse thermal environment for improvements [19, 20]. To investigate the impact of the crop canopy under the active heat storage and release system, Ke Xinglin [21, 22] et al. developed the sixth-generation active heat storage and release system based on the fourth-generation system and conducted demonstration applications. Overall, research on heat retention and thermal environments in solar greenhouses in China primarily focuses on [23-25]: (1) Built-in or external forms are used to store more heat during the day through different heat storage methods and release it into the greenhouse at night to raise the room temperature, realizing the transfer of heat in time and in space. (2) By testing indoor environmental temperature and heat flux, a comparative analysis of the microclimate environments of solar greenhouses with different structural types and materials is conducted, thereby evaluating the thermal and light performance of the solar greenhouses. (3) Based on the theory of mass-energy balance and heat transfer, we quantitatively describe the heat transfer process inside the solar greenhouse, establish a simulation model of the solar greenhouse environment, and then use the model to optimize the structural parameters of the greenhouse and the selection of materials.

Current research has proposed some methods to increase the heat storage capacity of solar greenhouses, mostly in the form of passive heat storage, and some ac-

tive heat storage methods such as solar collectors are difficult to popularize due to the high cost. The active heat storage and release system is a kind of cheap and convenient solar greenhouse heat control equipment, but its related theory and engineering parameters need to be further improved. Through this experimental study, the role of water flow in the active heat storage and release system within solar greenhouses is explored, providing theoretical and practical support for the promotion and application of active heat storage and release system. Ultimately, this research aims to optimize greenhouse structures and reduce carbon emissions.

# 2 Materials and Methods

## 2.1 Description of the Experiments

The experimental greenhouse is located in the Comprehensive Experimental Laboratory of the Facility Agriculture Science and Engineering Department at Sichuan Agricultural University, Chengdu campus. The solar greenhouse measures 50 meters in length, 3 meters in height, and 8 meters in span.

## 2.2 Structure and Working Principle of the Active Heat Storage and Release System

The structure of the active heat storage and release system consists of three components: the heat collection device, the heat storage device, and the control device.

The main composition of the system's heat collection device is a double-layer black plastic film, the test water in the pumping pump under the action of flowing down the film. The heat storage tank as a system of heat storage device, the outer surface of its surrounding foam board insulation layer, the volume of the tank is 0.27 m³, control device consists of a water pump, inlet and return piping and controllers, the pump selection of single-phase submersible electric pumps, the power of 0.37 kW. active storage and release of heat system of the main parameters as shown in Table 1.

## 2.3 Pilot Test Program

The active heat storage and release system is installed in the experimental greenhouse. The indoor air temperature measurement point is located at the geometric center of the greenhouse, at a height of 1 meter above the ground. The outdoor air temperature measurement point is also positioned at a height of 1 meter above the ground. The water temperature measurement point is located at the geometric center of the water tank. The indoor solar radiation irradiance measurement point is located on the outer surface of the heat collection device, with a height of 2.0 meters above the ground. The outdoor solar radiation irradiance measurement point is also positioned at a height of 2.0 meters. The temperature sensors used in the experiment are T-type thermocouples. Prior to the experiment, the instruments require treatment for radiation protection and rust prevention. Data acquisition and storage are conducted using a data acquisition instrument (TP1708P), with a data collection interval set to 10 minutes. Six different flow rates (0.7, 0.8, 0.9, 1.0, 1.1, and 1.2 $m^3 h^{-1}$) are set on the heat collection panel, with the initial inlet water temperature controlled at 15 ℃. The system's heat storage operation is scheduled from 9:00 AM to 4:00 PM during the day, while the heat release operation is set for the night from 12:30 AM to 6:00 AM.

Table 1 Main engineering structure parameters of Active Heat Storage and Release System

| Parameters | Units | Value |
|---|---|---|
| Collector plate length | m | 2.4 |
| Collector plate height | m | 1.8 |
| Thermal insulation board thickness | m | 0.03 |
| Water supply pipe diameter | m | 0.05 |
| Perforated pipe diameter | m | 0.032 |
| Return pipe diameter | m | 0.16 |
| Hole diameter of perforated pipe | m | 0.0032 |
| Thermal conductivity of insulation board | $w (m k)^{-1}$ | 0.030 |
| Light transmittance of light-transmitting layer | % | 87 |
| Thermal storage tank volume | $m^3$ | 0.27 |

## 2.4 Experimental Instruments

The U23-001 type automatic temperature and humidity recorder has a temperature accuracy of ± 0.2 ℃, with a measurement range of -30 to 50 ℃. The humidity accuracy is ±3%, with a measurement range of 0 to 100%.

Light sensor type JXBS - 3001 - GZ with an accuracy of ±5%.

TP1708P Data Collector.

Intelligent Flow Accumulator (Model HLK801).

Turbine flow meters (HL - LW series).

T-type thermocouples are deployed at the temperature

measurement points of the inlet and outlet water sections and are connected to the data acquisition device. The data acquisition device records data at 10-minute intervals.

# 3 Results and Analysis

## 3.1 Calculation of Overall Heat Transfer Coefficient

The combined heat transfer coefficient h between the collector plate and the greenhouse was calculated for six operating flow rates according to Eq.

Instantaneous heat collection by daytime collector units:

$$Q = C_W \rho_W q T \Delta t \quad (1)$$

$$Q = I + hs(t_a - t_w) \quad (2)$$

In the equation, Q——Instantaneous heat collection of the collector unit, J

$C_w$——Specific heat capacity of water, $4.2\times10^3$ J (kg ·℃)$^{-1}$

$\rho_w$——Density of water, 1000 kg m$^{-3}$

Δt——Temperature Difference of Inlet and Outlet Water in the Storage Tank, ℃

T——Time Required for Water to Flow Through the Heat Collection Panel, s

q——Volumetric Flow Rate of Water, kg s$^{-1}$

I——Solar Radiation Intensity, W m$^{-2}$

S——Unit Area of the Heat Collection Unit, m$^2$

$t_a$——Air Temperature, ℃

$t_w$——Average Temperature of Inlet and Outlet Water, ℃

After establishing the theoretical model, a calculation model for the overall heat transfer coefficient can be obtained:

$$h = \frac{2}{L \cdot x} \varphi_v \cdot \rho \cdot C_p \cdot \ln \frac{T_n - T_a}{T_{in} - T_a} \quad (3)$$

The overall heat transfer coefficient between the heat collection panel and the greenhouse under different operating flow rates can be obtained from Formula (3). The calculation results are shown in Table 2.

After calculation, the variation of the overall heat transfer coefficient of the system at different flow rates is shown in Table 2. When the inlet water temperature is controlled at 15 ℃, the overall heat transfer coefficient of the active heat storage and release system continuously increases when the water flow rate is less than 1.0 m$^3$h$^{-1}$. When the water flow rate is equal to or greater than 1.0 m$^3$h$^{-1}$, the overall heat transfer coefficient of the system no longer changes. The control of the water flow rate is driven by the pump, with higher power resulting in increased flow velocity. By maintaining the flow rate at 1.0 m$^3$h$^{-1}$, the system minimizes energy consumption while ensuring optimal heat transfer, thus achieving both economic efficiency and energy savings.

Table 2 Comprehensive heat transfer coefficient under different flow rates

| **Flow volume (m$^3$h$^{-1}$)** | **0.7** | **0.8** | **0.9** | **1.0** | **1.1** | **1.2** |
|---|---|---|---|---|---|---|
| Calculated value of comprehensive heat transfer coefficient (W (m$^2$ ·℃)$^{-1}$) | 20 | 23 | 26 | 27 | 27 | 27 |

## 3.2 Validation of the Water Temperature Prediction Model

$$T_{n+1} = T_n + \frac{V}{\varphi_v}\left(\left(T_n - T_a - \frac{\eta}{h} I\right) e^{-\frac{hLx}{2\varphi_v \rho C_p}} + T_a + \frac{\eta}{h} I - T_n\right) \Delta t \quad (4)$$

The water temperature prediction model (4) can be derived from the instantaneous heat collected by the heat-collecting unit and related thermodynamic equations. By inputting the relevant parameters at time $T_n$ the model can calculate the temperature at the next time point $T_{n+1}$. Consequently, equation (4) can be used to simulate the water temperature within the heat storage tank at various times throughout the day. The system can be shut down when the maximum temperature is reached, thereby achieving the highest amount of collected heat.

Using MATLAB software, the initial temperature during the daytime heat-collecting operation is input to obtain the water temperatures at various time points during the daytime heat-collecting phase for different flow rates. These predicted values are then compared with the measured values to validate the model.

Figure 1 shows the relationship between the simulated and measured values of the tank water temperature for the heat collection phase of the daytime operation of the

active heat storage and release system at a flow rate of 0.7 m $^3$h$^{-1}$. The figure indicates that the solar radiation intensity indoors follows a trend of first increasing and then decreasing over time, with the indoor air temperature reaching its maximum value of 36.1 ℃ at 1:00 PM; The solar radiation intensity reaches its maximum value of 339.5 W m$^{-2}$ at 12:30 PM. Both the measured and simulated values of the water temperature in the tank exhibit a trend of first increasing and then decreasing. The measured value reaches its maximum of 27.4 ℃ at 3:30 PM, while the simulated value peaks at 26.4 ℃ at 3:40 PM. The maximum relative error between the measured and simulated values is 12.00%, the minimum relative error is 3.10%, and the average relative error is 6.91%.

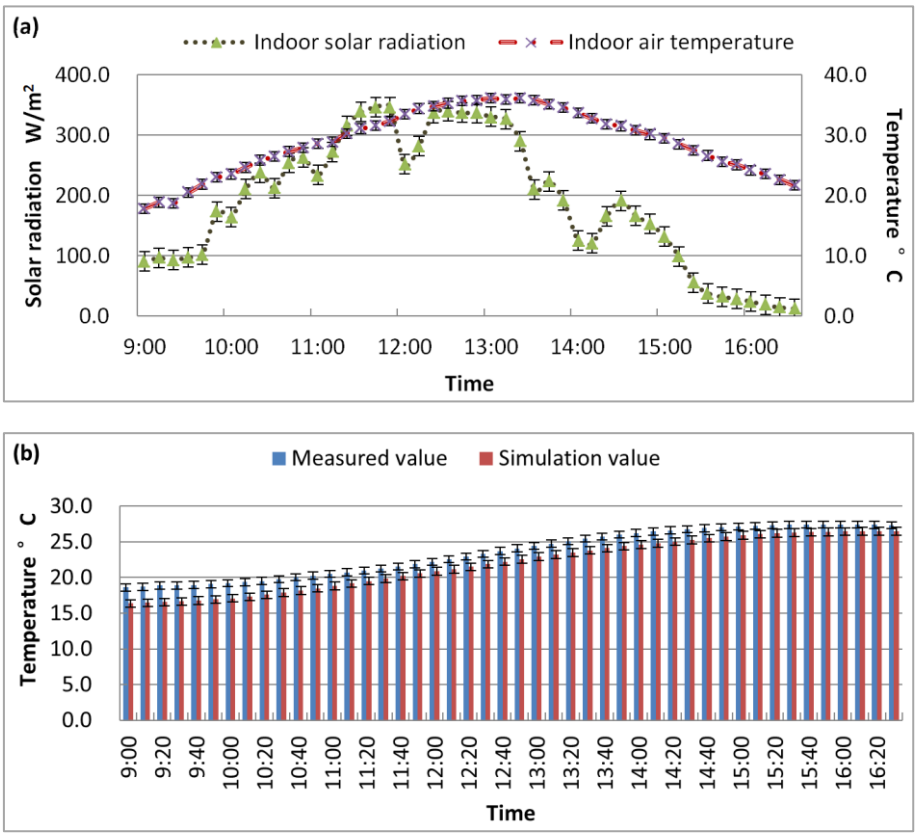


Figure 1 The water temperature changes with time in the heat collection stage at a flow rate of 0.7 m $^3$h$^{-1}$

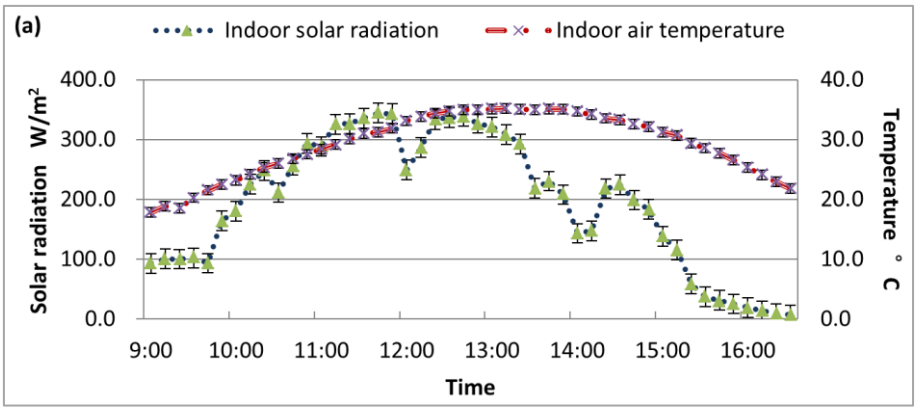

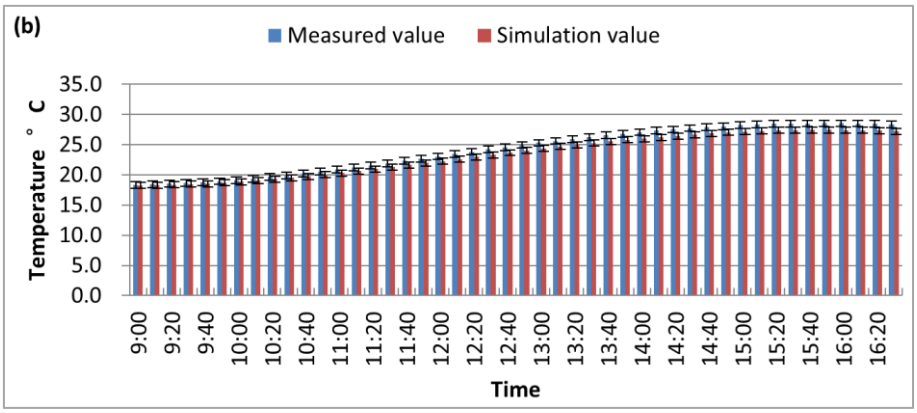


Figure 2 The water temperature changes with time in the heat collection stage at a flow rate of 0.8 m $^3$h$^{-1}$

Figure 2 shows the relationship between the simulated and measured values of the tank water temperature for the heat collection phase of the daytime operation of the active heat storage and release system at a flow rate of 0.8 m $^3$h$^{-1}$. From the figure, it can be observed that both the indoor air temperature and solar radiation intensity exhibit a trend of initially rising and then falling over time, with the indoor air temperature reaching a maximum of 35.1 ℃ at 1:00 PM. The solar radiation intensity reached its maximum of 338.3 W m$^{-2}$ at 12:40 PM. The measured and simulated water temperatures in the tank both exhibited a trend of initially rising and then falling, with the measured value reaching a maximum of 28.5 ℃ at 3:20 PM, while the simulated value peaked at 27.4 ℃ at the same time. The maximum relative error between the measured and simulated values was 4.05%, the minimum relative error was 0.44%, and the average relative error was 3.06%.

Figure 3 shows the relationship between the simulated and measured values of the tank water temperature for the heat collection phase of the daytime operation of the active heat storage and release system at a flow rate of 0.9 m $^3$h$^{-1}$. From the figure, it can be observed that both the indoor air temperature and solar radiation intensity exhibit a trend of initially rising and then declining over time. The indoor air temperature reaches its maximum value of 33.7 ℃ at 1:00 PM, while the solar radiation intensity peaks at 388.5 W m$^{-2}$ at 11:10 AM. The measured and simulated values of the water temperature in the water tank both exhibit a trend of initially rising and then declining. The measured value reaches its maximum of 29.9 ℃ at 3:50 PM, while the simulated value peaks at 27.6 ℃ at 3:40 PM. The maximum relative error between the measured and simulated values is 7.97%, the minimum relative error is 1.04%, and the average relative error is 6.00%.

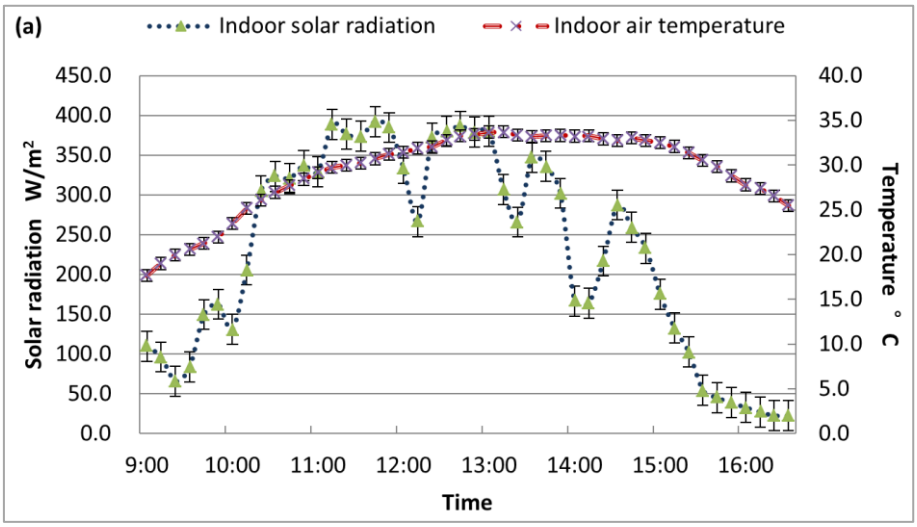

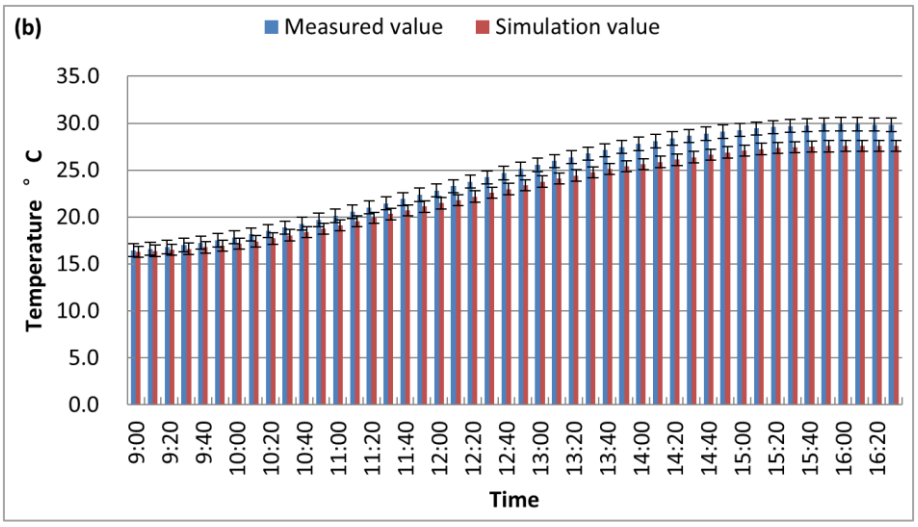


Figure 3 The water temperature changes with time in the heat collection stage at a flow rate of 0.9 m $^3$h$^{-1}$

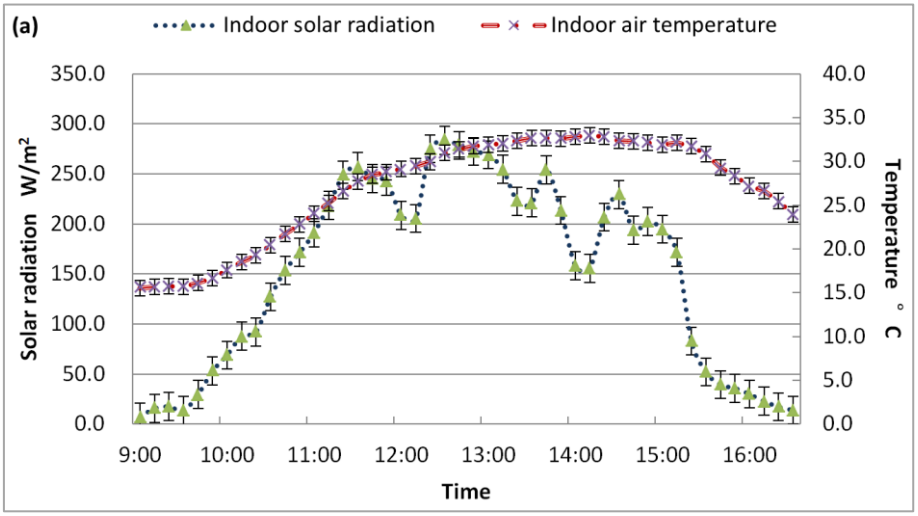


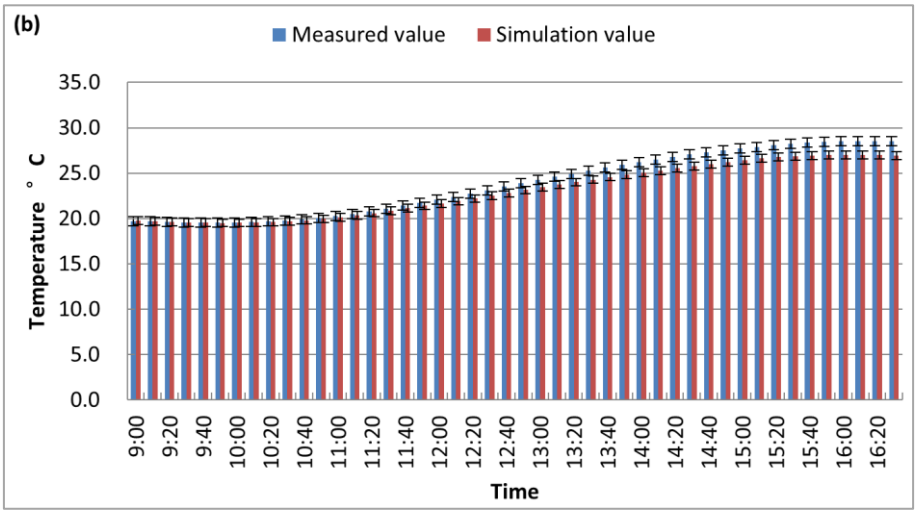


Figure 4 The water temperature changes with time in the heat collection stage at a flow rate of 1.0 m $^3$h$^{-1}$

Figure 4 shows the relationship between the simulated and measured values of the tank water temperature for the

heat collection phase of the daytime operation of the active heat storage and release system at a flow rate of 1.0 m $^3$h$^{-1}$. The indoor air temperature and solar radiation intensity exhibit a trend of initially rising and then declining over time. The indoor air temperature reaches its maximum of 32.7 ℃ at 1:30 PM, while the solar radiation intensity peaks at 12:30 PM, measuring 283.4 W m$^{-2}$. The measured and simulated values of the water temperature in the water tank also follow a similar pattern, with the measured value reaching a maximum of 28.5 ℃ at 4:00 PM, and the simulated value peaking at 27.0 ℃ at 3:50 PM. The maximum relative error between the measured and simulated values is 5.42%, the minimum relative error is 0.05%, and the average relative error is 2.70%.

Figure 5 shows the relationship between the simulated and measured values of the tank water temperature for the heat collection phase of the active heat storage and release system operating during the daytime at a flow rate of 1.1 m $^3$h$^{-1}$. The indoor air temperature and solar radiation intensity exhibit a trend of initially rising and then declining over time. The indoor air temperature reaches its maximum of 35.1 ℃ at 1:00 PM, while the solar radiation intensity peaks at 11:40 AM, measuring 344.4 W m$^{-2}$. The measured and simulated values of the water temperature in the water tank also follow a similar pattern, with the measured value reaching a maximum of 28.5 ℃ at 4:00 PM and the simulated value peaking at 27.4 ℃ at 3:30 PM. The maximum relative error between the measured and simulated values is 13.45%, the minimum relative error is 0.80%, and the average relative error is 3.99%.

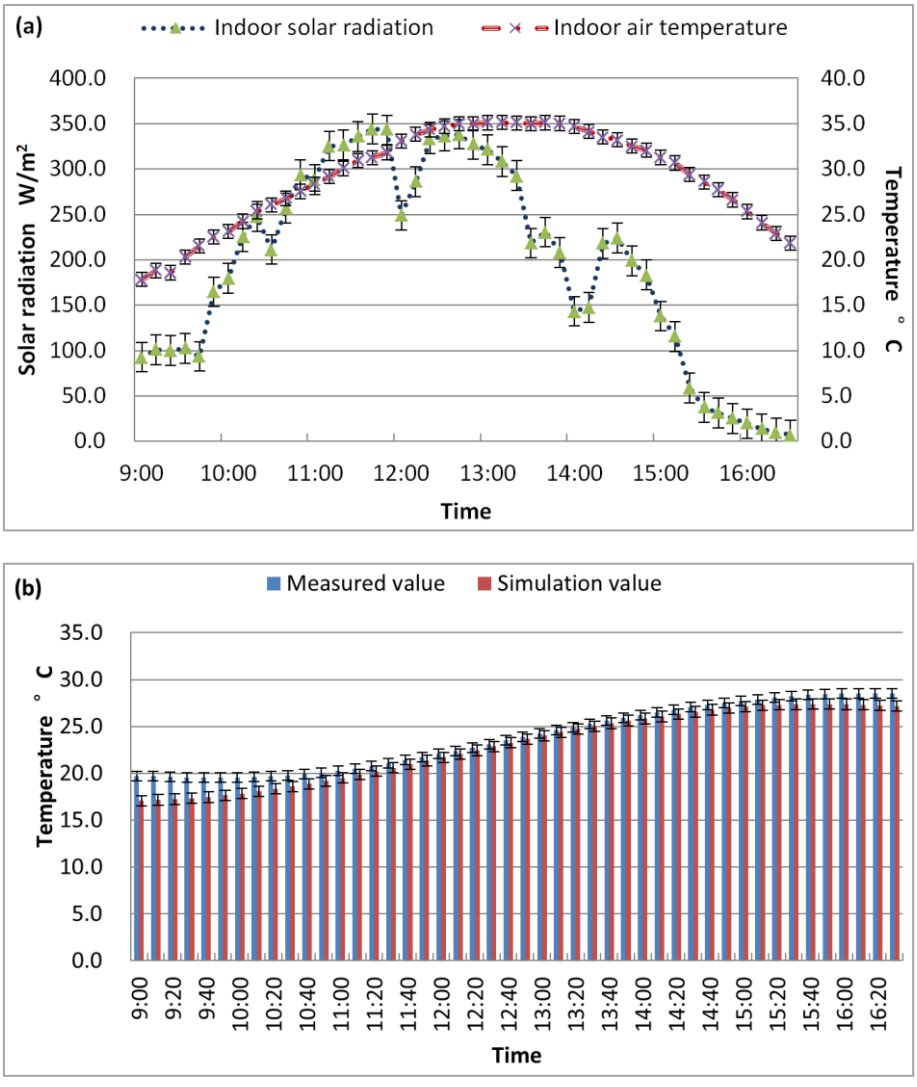


Figure 5 The water temperature changes with time in the heat collection stage at a flow rate of 1.1 m $^3$h$^{-1}$

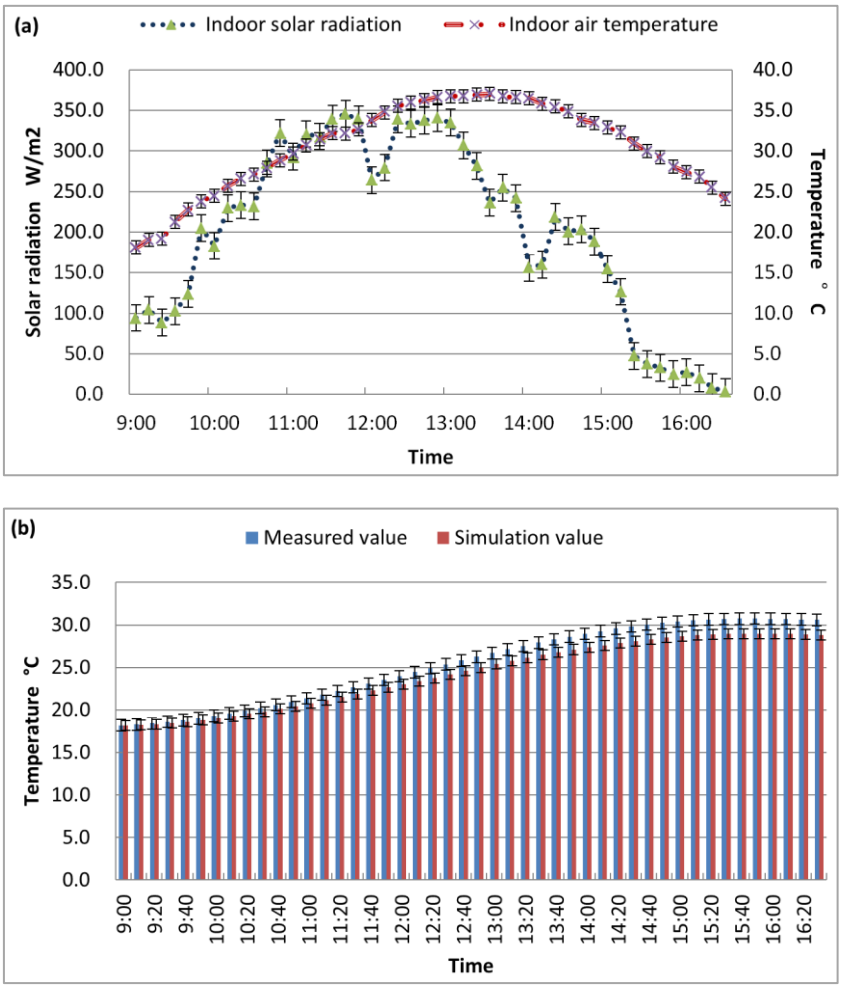


Figure 6 The water temperature changes with time in the heat collection stage at a flow rate of 1.2 m $^3$h$^{-1}$

Figure 6 shows the relationship between the simulated and measured values of the tank water temperature for the heat collection phase of the daytime operation of the active heat storage and release system at a flow rate of 1.2 m $^3$h$^{-1}$. The indoor air temperature and solar radiation intensity show a trend of initially rising and then declining over time. The indoor air temperature reaches its maximum of 37 ℃ at 1:30 PM, while the solar radiation intensity peaks at 11:40 AM, measuring 345.6 W m$^{-2}$. The measured and simulated values of the water temperature in the tank also exhibit a similar pattern, with the measured value reaching a maximum of 30.7 ℃ at 3:50 PM and the simulated value peaking at 29.0 ℃ at 3:40 PM. The maximum relative error between the measured and simulated values is 5.94%, the minimum relative error is 0.03%, and the average relative error is 3.99%.

In summary, it can be obtained that, based on the model simulation of six different flow rates of the system under the daytime collector stage of the tank water temperature, compared with the measured values, the average relative error is in the range of 2.70% ~ 6.91% (such as Table 3).

Table 3 Comparison of the average relative error between simulated and measured water temperature values at different flow rates

| **Flow volume (m $^3$h$^{-1}$)** | **0.7** | **0.8** | **0.9** | **1.0** | **1.1** | **1.2** |
|---|---|---|---|---|---|---|
| Average relative error (%) | 6.91 | 3.06 | 6.00 | 2.70 | 3.99 | 3.99 |

# 4. Conclusions

Based on the results of this experimental study, the following conclusions can be drawn.

First, in the control of the inlet water temperature is the same, the active storage and Release system inlet water flow rate is less than 1.0 m $^3$h$^{-1}$, with the increase in flow rate of the integrated heat transfer coefficient continues to rise; flow rate of more than 1.0 m $^3$h$^{-1}$ integrated heat

transfer coefficient stabilized at 27 W $(m^2 \cdot ℃)^{-1}$. When the flow rate is set to 1.0 $m^3 h^{-1}$ not only to get the maximum integrated heat transfer coefficient, and at the same time reduces the system energy consumption, improve the system economy. energy consumption, improving the economy of the system.

Secondly, the average relative error between the simulated and measured values of water temperature in the collector stage calculated by the model is 2.70% ~ 6.91%, which proves that the experimental model is established correctly and can be based on the model to predict the trend of water temperature on the same day. Also at a flow rate of 1.0 $m^3 h^{-1}$, the average relative error between the simulated and measured values was the lowest at 2.70%.

Third, according to the analysis of the test results, the daily change of the water temperature of the heat storage tank has a delay relative to the indoor air temperature and the change of solar radiation intensity.

The model established in this test can predict the daily change of the water temperature of the heat storage tank, optimize the existing time control mode, so that the system stops running when the water temperature reaches the highest value, reduce the loss of heat storage, obtain the maximum amount of heat collection, save the system operating costs, and improve the energy efficiency of the system. As the system's test time is not long, it is still in the primary stage of the test, the next step of the research will optimize the system engineering structure parameters, improve the engineering assembly process, further improve the performance of the active heat storage and release system, refine the heat storage effect that can be achieved by the system, and lay the technical foundation for the large-scale promotion of greenhouse active energy storage and temperature control equipment.

## References

[1] Tong GH, David MC. Temperature variations in energy storage layers in Chinese solar greenhouse walls [J]. *Trans Chin Soc Agric Eng*, 2019, 35(7): 170-177.

[2] Bao EC, Cao YF, Zou ZR, Shen TT, Zhang Y. Research progress of thermal storage technology in energy-saving solar greenhouse [J]. *Trans Chin Soc Agric Eng*, 2018, 34(6): 1-14.

[3] Wang W, Wang JJ, Xiao Y. Vegetable cultivation techniques in high-efficiency and energy-saving sunlight greenhouse [J]. *Contemp Hortic*, 2018(10): 38.

[4] Zhao P, Song MJ. Test and analysis of the modular cotton-polyester wall solar greenhouse thermal performance [J]. *J Chin Agric Mech*, 2018, 39(6): 44-47, 70.

[5] Luo QL, Cheng RF, Zhang Y, Fang H, Li D, Zhang JF, Song GX. Optimization of active heat storage and release system in solar greenhouse [J]. *Trans Chin Soc Agric Eng*, 2020, 36(17): 234-241.

[6] Wang YX, Liu S, Wang PZ, Shi GY. Preparation and characterization of microencapsulated phase change materials for greenhouse application [J]. *Trans Chin Soc Agric Mach*, 2016, 47(09): 348-358.

[7] Jiang ZP, Tie SN. Property and heat storage performances of Glauber's salt-based phase change materials for solar greenhouse in Qinghai-Tibet plateau [J]. *Trans Chin Soc Agric Eng*, 2016, 32(20): 209-216.

[8] Benli H, Durmus A. Performance analysis of a latent heat storage system with phase change material for new designed solar collectors in greenhouse heating [J]. *Sol Energy*, 2009, 83(12): 2109-2119.

[9] Berroug F, Lakhal EK, El OM, M. F, H. EQ, Thermal performance of a greenhouse with a phase change material north wall [J]. *Energy Build*, 2011, 43(11): 3027-3035.

[10] Peng DL. Research on process simulation and structure optimization of heat storage and release of solar greenhouse wall [D]. Beijing, Chinese Academy of Agricultural Sciences, 2014.

[11] Li M, Zhou CJ, Wei XM. Thickness determination of heat storage layer of wall in solar greenhouse [J]. *Trans Chin Soc Agric Eng*, 2015, 31(2): 177-183.

[12] Lu W, Zhang Y, Fang H, Yang Q. Modelling and experimental verification of the thermal performance of an active solar heat storage-release system in a Chinese Solar Greenhouse [J]. *Biosyst Eng*, 2017, 160, 12-24.

[13] Fang H, Yang QC, Liang H, Wang S. Experiment of temperature rising effect by heat release and storage with shallow water in solar greenhouse [J]. *Trans Chin Soc Agric Eng*, 2011, 27(5): 258-263.

[14] Zhang Y, Yang QC, Fang H. Research on warming effect of water curtain system in Chinese solar greenhouse [J]. *Trans Chin Soc Agric Eng*, 2012, 28(4): 188-193.

[15] Liang H, Fang H, Yang QC, Zhang Y, Sui WT. Performance testing on warming effect of heat storage-release curtain of back wall in Chinese solar greenhouse [J]. *Trans Chin Soc Agric Eng*, 2013, 29(12): 187-193.

[16] Sun WT, Yang QC, Fang H, Zhang Y, Guan DP, Lu W. Application of heating system with active heat storage-release and heat pump in solar greenhouse [J]. *Trans Chin Soc Agric Eng*, 2013, 29(19): 168-177.

[17] Zhou S, Zhang Y, Cheng RF, Yang QC, Fang H, Zhou B, Lu W, Zhang F. Evaluation on heat preservation effects in micro-environment of large-scale greenhouse with active heat storage system [J]. *Trans Chin Soc Agric Eng*, 2016, 32 (6): 218-225.

[18] Fang H, Yang QC, Zhang Y, Sun WT, Lu W, Liang H. Performance of a solar heat collection and release system for improving night temperature in a Chinese solar greenhouse [J]. App*l Eng Agric*, 2015, 31(2): 283-289.

[19] Zhou B, Zhang Y, Fang H, Yang Q, Ao H. *Performance experiment and design of simply assembled Chinese solar greenhouse equipped with heating and dehumidification system* [J]. *Trans Chin Soc Agric Eng*, 2016, 32(11): 226-232.

[20] Ma QL, Yang QC, Ke XL, Zhang Y, He YK, Zhan ZP, Jin YF. Performance of an active heat storage-release system for canopy warming in solar greenhouse [J]. *J Northwest A&F Univ*, 2020, 48(01): 57-64.

[21] Ke XL, Yang QC, Zhang Y, Fang H, He YK, Zhang C. Warming effect comparison between substrate warming system and air warming system by active heat storage-release in Chinese solar greenhouse [J]. *Trans Chin Soc Agric Eng*, 2017, 33(22): 224-232.

[22] Ke XL. Study on the High-efficiency Utilization Mechanism of Actively Stored and Released Heat Energy in Sunlight Greenhouse [D]. Beijing: Chinese Academy of Agricultural Sciences, 2018.

[23] Tong XJ, Sui ZP, Li TL, Liu YL, Ma J. Heating Performance of Heating Device of the Solar Energy Water-Cycling System in Greenhouse [J]. *J Shenyang Agric Univ*, 2016, 47(01): 92-96.

[24] Xu WW, Ma CW, Song WT, Cheng YJ, Wang PZ. Test on heat-collecting performance of solar heat collection and release system with water cycling inside hollow plates in chinese solar greenhouse [J]. *Trans Chin Soc Agric Mach*, 2018, 49(07): 336-334.

[25] Ma CW, Jiang YC, Cheng JY, Zhao SM, Xia N, Wang PZ, Yang P. Analysis and experiment of performance on water circulation system of steel pipe network formed by roof truss for heat collection and release in Chinese solar greenhouse [J]. *Trans Chin Soc Agric Eng*, 2016, 32(21): 209-216.